PLOS ONE

RESEARCH ARTICLE

Distinct temporal dynamics of planktonic archaeal and bacterial assemblages in the bays of the Yellow Sea

Jong-Geol Kim[1], Joo-Han Gwak[1], Man-Young Jung[2], Sung-Uk An[3], Jung-Ho Hyun[3], Sanghoon Kang[4]*, Sung-Keun Rhee[1]*

1 Department of Microbiology, Chungbuk National University, Gaeshin-dong, Heungduk-gu, Cheongju, South Korea, **2** Department of Microbiology and Ecosystem Science, Division of Microbial Ecology, University of Vienna, Althanstrasse, Vienna, Austria, **3** Department of Marine Sciences and Convergent Technology, Hanyang University, Hanyangdaehak-ro Ansan, Gyeonggi-do, South Korea, **4** Department of Biological Sciences, Eastern Illinois University, Charleston, IL, United States of America

* rhees@chungbuk.ac.kr (SKR); Sanghoon_Kang@baylor.edu (SK)

Citation: Kim J-G, Gwak J-H, Jung M-Y, An S-U, Hyun J-H, Kang S, et al. (2019) Distinct temporal dynamics of planktonic archaeal and bacterial assemblages in the bays of the Yellow Sea. PLoS ONE 14(8): e0221408. https://doi.org/10.1371/journal.pone.0221408

Editor: Zhe-Xue Quan, Fudan University, CHINA

Received: April 10, 2019

Accepted: August 6, 2019

Published: August 26, 2019

Data Availability Statement: All sequence data are available from the GenBank database (accession number PRJNA448352).

Funding: This work was supported by the Research Year of Chungbuk National University in 2019, C1 Gas Refinery Program (NRF-2015M3D3A1A01064881) and the framework of international cooperation program (2018K2A9A2A06021751N) managed by the National Research Foundation of Korea, and the project titled "Long-term change of structure and function in marine ecosystems of Korea," funded

Abstract

The Yellow Sea features unique characteristics due to strong tides and nutrient-enriched freshwater outflows from China and Korea. The coupling of archaeal and bacterial assemblages associated with environmental factors at two bay areas in the Yellow Sea was investigated. Temporal variations of the archaeal and bacterial assemblages were shown to be greater than the spatial variations based on an analysis of the 16S rRNA gene sequences. Distinct temporal dynamics of both planktonic archaeal and bacterial assemblages was associated with temperature, NO_2^-, and chlorophyll a ([chl-*a*]) concentrations in the bays of the Yellow Sea. The [chl-*a*] was the prime predictor of bacterial abundance, and some taxa were clearly correlated with [chl-*a*]. *Bacteroidetes* and *Alpha-proteobacteria* dominated at high [chl-*a*] stations while *Gamma-proteobacteria* (esp. SAR86 clade) and *Actinobacteria* (*Candidatus* Actinomarina clade) were abundant at low [chl-*a*] stations. The archaeal abundance was comparable with the bacterial abundance in most of the October samples. Co-dominance of Marine Group II (MGII) and *Candidatus* Nitrosopumilus suggests that the assimilation of organic nitrogen by MGII could be coupled with nitrification by ammonia-oxidizing archaea. The distinct temporal dynamics of the archaeal and bacterial assemblages might be attributable to the strong tides and the inflow of nutrient-rich freshwater.

Introduction

Archaea and bacteria actively react to changes in environmental conditions due to their large abundance, great diversity, and fast growth. Archaeal and bacterial assemblages thus provide essential perspectives for understanding the functions of archaea and bacteria in terms of their ecosystem services in marine ecosystems [1, 2].

Bacteria are a major component in microbial food webs and biogeochemical cycles in marine ecosystems [1, 3]. Furthermore, molecular approaches have revealed that archaea, in

by the Ministry of Oceans and Fisheries. J.-G. K. was supported by the Young Researcher Supporting Program (NRF-2017R1C1B1011324). The funders had no role in study design, data collection and analysis, decision to publish, or preparation of the manuscript.

Competing interests: The authors have declared that no competing interests exist.

addition to bacteria, are also abundant planktonic microbial components, and advances in omics approaches have revealed that planktonic archaea have major roles in biogeochemical cycles including the nitrogen and carbon cycles [4–8]. Ammonia-oxidizing archaea, which used to be called Marine Group I, belong to *Thaumarchaeota* and have become increasingly abundant at greater depths [4, 9, 10]. Considerable progress has been made in the physiology, biochemistry, and ecological functions of ammonia-oxidizing archaea belonging to *Ca*. Nitrosopumilus of *Thaumarchaeota* [6, 11, 12]. Three groups of *Euryarchaeota* are less known due to the lack of available isolates in these groups. MGII of *Euryarchaeota* [13] has generally been observed to dominate in archaeal communities of the surface ocean and is predicted to have heterotrophic life styles. However, the mechanisms controlling the distribution of *Archaea* in different water columns of the ocean remain elusive.

The Yellow Sea (YS) features unique oceanographic characteristics. For example, strong currents/tides and nutrient-enriched freshwater outflows from China and Korea contribute to localized phytoplankton blooms along the coastal areas of the YS. Furthermore, the YS is considered one of the most complicated continental sea areas in the world because the seasonal variations of the currents, air temperature, river runoff, and wind stress in this shallow sea generate a high variability in temperature and salinity [14]. Research on the changes in the YS environmental factors during a 25-year period of the last century suggested clear trends for nutrient concentrations [15], which might be associated with industrial and agricultural wastes through run-off and atmospheric deposition into the sea as well as the changing climate [15, 16]. The change in nutrient concentrations and stoichiometry consequently can be associated with the increasing frequency of algal blooms and hypoxic dead zones, which are related to changes in the prokaryote community structure and dynamics [17].

The archaeal and bacterial community composition associated with phytoplankton blooms in the coastal waters of the YS near Korea has not to our knowledge been documented at the taxa-specific level using next generation sequencing. In this study, we carried out temporal water sampling at two bay areas on the west coast of the Korean Peninsula over one year to investigate the archaeal and bacterial assemblages associated with the environmental factors. Distinct archaeal and bacterial assemblages were observed at the bay areas on the west coast of the Korean Peninsula. Dynamic temporal changes in the archaeal and bacterial assemblages were observed with an archaeal bloom composed of *Ca*. Nitrosopumilus and MGII in autumn (October). Environmental factors including temperature, NO_2^-, and [chl-*a*] were identified to be associated with changes of the archaeal and bacterial assemblages. The findings contribute to our knowledge of patterns of temporal changes of prokaryotic assemblages in coastal seawaters.

Materials and methods

Ethics statement

No specific permissions were required for collection of surface seawater samples from two bays called Garorim and Gyeonggi on the west coast of the Korean Peninsula since these locations are not protected area. We confirm that the field studies did not involve endangered or protected species.

Site description and sampling

Surface seawater samples were collected from two bays called Garorim (GR) and Gyeonggi (GI) on the west coast of the Korean Peninsula (Fig 1 and Table A in S1 Appendix) as part of the Korean Long-term Marine Ecological Research Program, which was conducted in April, July, and October of 2015 and in February 2016. The major difference between the two bays is that Garorim Bay has no large inputs of freshwater whereas Gyenonggi Bay is affected by

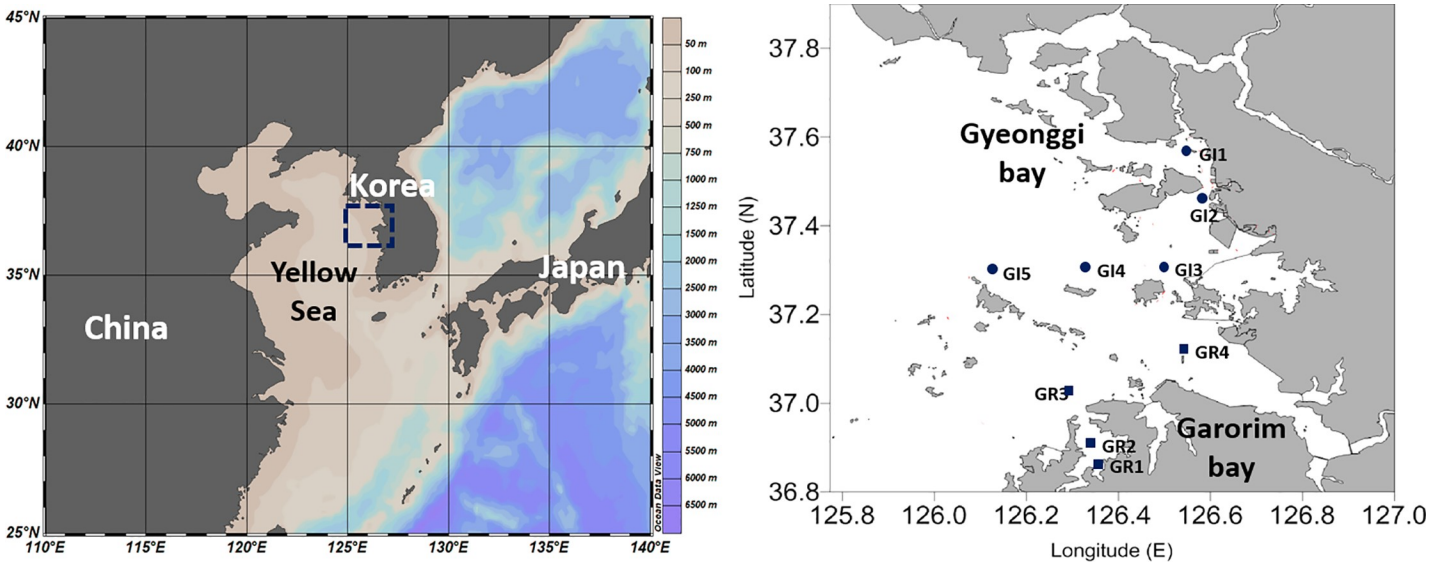

Fig 1. Location of sampling sites in two bay areas in the Yellow Sea.

https://doi.org/10.1371/journal.pone.0221408.g001

freshwater discharged from the Han River. Each seawater sample (2 L) was filtered immediately through a Whatman GF/A filter (pore size: 1.6 μm, diameter: 45mm) to remove any suspended particles and eukaryotes [18–20] before being filtered through a 0.22 μm pore-size filter (diameter: 45mm, Supor polyethersulfone, Pall Life Sciences) to capture the archaeal and bacterial cells using a vacuum pump. The filters were preserved at -80˚C until DNA extraction, which was performed after enzymatic lysis and phenol:chloroform purification [21]. The concentration of DNA was determined using a Nano-Drop ND-1000 spectrophotometer (Nano-Drop Technologies, Wilmington, DE).

Seawater properties

Water temperature, salinity, pH, and dissolved oxygen (DO) were measured *in situ* using a Multi-Parameter Sonde (YSI-6600V2: YSI, Yellow springs, OH, USA). Seawater samples were immediately transferred to the laboratory to analyze other properties of the water. SPM (suspended particulate matter) was determined by filtering the material in a known volume of the sample onto pre-weighed filter papers (GF/F, Whatman, Maidstone, UK). Filters were washed with fresh water and then dried and weighed. Particulate organic carbon (POC) was determined for samples filtered through pre-combusted GF/F filters, which were dried and measured using a CHNS analyzer (Carlo Erba, Val de Reuil, France). The concentrations of the major inorganic nutrients (NH_4^+, NO_2^-, NO_3^-, PO_4^{2-}, and silicate) were analyzed using a Bran and Luebbe model Quatro AA (Auto Analyzer) according to the manufacturer's instructions. The dissolved organic carbon (DOC) measurements were carried out by a high-temperature catalytic oxidation technique (HTCO), as described in Suzuki, Tanoue [22], using a TOC-VCPH (Shimazu, Kyoto, Japan). The total [Chl-*a*] concentration was determined using a spectrophotometer after extracting the filter with 90% acetone at 4˚C for 24h in the dark [23].

Quantification of bacterial and archaeal 16S rRNA genes

Bacterial and archaeal 16S rRNA gene copies were quantified using a MiniOpticon real-time PCR detection system (BIO-RAD, Hercules, California, USA) and the built-in Opticon Monitor Software version 3.1 (Bio-Rad Laboratories, Hercules, CA, USA). The bacterial and

archaeal 16S rRNA genes were amplified using the archaea-specific primer set 519F-727R and the bacteria-specific primer set bac518F-bac786R as described by Park and colleagues [24]. The real-time PCR efficiencies of the bacterial and archaeal 16S rRNA gene assays were 90–95% and 92–96%, respectively, with r^2 values of $\geq$ 0.99 in all assays. The following thermal cycling parameters were used to amplify all genes: 15 min. at 95˚C followed by 40 cycles of 20 s at 95˚C, 20 s at 55˚C and 20 s at 72˚C, and readings were taken between each cycle. Standard curves were prepared in each run using standards of reference genes (archaeal 16S rRNA gene, DQ831586; bacterial 16S rRNA gene, FJ656473, respectively) at abundances ranging from 10^3 to 10^8 gene copies per reaction. These curves were used to estimate gene abundance in the seawater samples. The r^2 value for the standard curve was 0.99, and the slope value was −3.14, giving an estimated amplification efficiency of 93%. The specificity of real-time PCRs was tested by analyzing melting curves, checking the sizes of reaction products using gel electrophoresis, and sequencing of the reaction products [25].

PCR amplification and pyrosequencing of the prokaryotic 16S rRNA genes

PCR amplifications of prokaryotic (bacterial and archaeal) 16S rRNA genes including the V4 and V8 hypervariable regions were done with the prokaryotic universal primers 787F (5′-ATTAGATACCCNGGTAG-3′) [26] and 1391R (5′-ACGGGCGGTGWGTRC-3′) primer set [27]. PCR was performed using 25 μl of 2× PCR Master Mix Solution (Intron, Seongnam, Korea), 1 μM of each primer (final concentration) and ca 10 ng of genomic DNA as the template, and water was added to a final volume of 50 μl. The following PCR cycles were used: initial denaturation at 94˚C for 5 min. followed by 30 cycles of 94˚C for 50 s, 55˚C for 30 s and 72˚C for 50 s and a final extension step at 72˚C for 6 min. The amplification products from each sample were purified using a PCR purification Kit (Cosmo4, Seoul, Korea). The DNA was quantified using a spectrophotometer (Nanodrop Technologies, Rockland, DE, USA) and was then mixed in equivalent proportions. Sequencing was performed using an GS FLX Titanium Genome Sequencer (454 Life Sciences, Branford, CT, USA). Multiplex identifiers (Roche, Basel, Schweiz), an adaptor and a short four-nucleotide sequence (TCAG), which were recognized by the system software and the priming sequences, were used to label the end fragments of the amplification products obtained from the samples by a sequencing provider (Macrogen, Seoul, Korea) according to the manufacturer's instructions.

Sequence analysis

Additional processing of the 16S rRNA gene sequences was done with QIIME 1.9.1 [28]. Paired-end reads were aligned using the fastq-join algorithm from ea-utils [29, 30]. Non-paired reads were discarded. The resulting sequences were then filtered at a Phred score of 20. Chimeric sequences were identified and removed using the UCHIME algorithm in USEARCH [31]. Open-reference OTU picking was done with uclust against the Greengenes 13_8 database [32] with a 0.97 similarity cutoff. Singletons were removed as the part of the OTU picking process. Sequences identified as chloroplasts or mitochondria and OUT with <1% abundance were then removed from the resulting OTU table by filtering. OTU tables for taxonomic groups specific to *Archaea* including MGII were extracted from the resulting complete data. New alignments and tree files were generated through QIIME specific to the new OTU tables. Sequence data that support the findings of this study have been deposited in GenBank with the BioProject accession code PRJNA448352.

Statistical analysis

All analyses were done in the R software package v. 3.3.1 [33] with appropriate packages (vegan, MASS, tree and ggplot2) and several custom scripts. Generalized linear modeling

(GLM) was done for the 16S rRNA gene copy number and the Shannon diversity index (*H*') of both the archaea and bacteria communities over a period of 1 year (February, April, July and October) from two different bays (GI and GR) with simultaneously measured environmental variables including physicochemical parameters (e.g., salinity, temperature, pH, etc.), environmental parameters (e.g., DOC, PON, NH_4^+, etc.) and biological parameters ([chl-*a*] and DO). The overall trends of the samples were assessed using non-metric multidimensional scaling (NMDS) ordination. Seasonal and spatial patterns were tested with permutational multivariate analysis of variance (PERMANOVA) and analysis of similarity (ANOSIM). Procrustes test with NMDS ordination configurations and the Mantel test were used to compare the archaeal and bacterial communities as well as the composite environmental variables. Redundancy analysis (RDA) models were constructed to describe the community structure ordination in linear environmental constraints following a similar procedure as that of the GLM for *H*'. Briefly, models were selected by a reduction approach from the full model based on multicollinearity (VIF) among the predictors (glm) and constraints (RDA) and by model comparison approaches based on information criterion (AIC and BIC). Environmental gradients were built on NMDS ordination using the vegan::ordisurf function which used generalized additive modeling (GAM) to overlay environmental variables in the ordination space [34]. The temperature and nitrite concentration gradient were selected by vector fitting to the NMDS ordinations.

Results

Environmental parameters

Salinity and other parameters at the GR stations (Table B in S1 Appendix) were more similar to each other due to a lack of freshwater inflow from land and the active tidal exchange of water with the open sea compared to those of GI stations (Fig 1). At the GI station, the salinity was lower at GI1 and GI2 where freshwater inflows from the Han River. The high SPM concentration was related to the tidal activity at both bays close to land and the inflow of the river at the GI stations. In addition, differences in other environmental factors such as pH, ammonia, and other nutrient concentrations support the influence of the freshwater inflows at GI1 and GI2. As appeared in Table B in S1 Appendix and Fig 2, the concentration of [Chl-*a*] shows strong spatial and seasonal variations. The winter (February) algal bloom was evident at the GR (GR1 and GR2) and GI (GI1 and GI2) stations close to land while the spring (April) algal bloom was observed at the GR (GR 3 and GR4) and GI (GI3 and GI5) stations close to ocean. It is interesting that during autumn (October), the nitrite concentration was especially high (1.5–4.2 μM) at the stations close to the open ocean such as GR3, GR4, GI3, GI4, and GI5.

Archaeal and bacterial abundance and diversity

The 16S rRNA gene copy number by qPCR and Shannon diversity index (*H*') of the operational taxonomic unit (OTU) obtained from pyrosequencing were used to estimate the abundance and diversity of the archaeal and bacterial communities, respectively (Figure A in S1 Appendix, Fig 3C and 3D, and Table C in S1 Appendix). The trend for the relative abundance of bacteria and archaea estimated by qPCR was mostly similar with that by pyrosequencing except for GR1 and GR2 in February. Bacterial abundance was higher than archaeal abundance in all of the February, April, and July samples. Unexpectedly, the archaeal abundance was comparable with the bacterial abundance in most of the October samples at both sites except for at GI1 and GI2 where seasonal freshwater influx existed (Figure A in S1 Appendix). In February, both the archaeal and bacterial abundance were significantly higher inside Garorim Bay (GR1 and GR2) (Figure A in S1 Appendix). The site variation diminished in the July

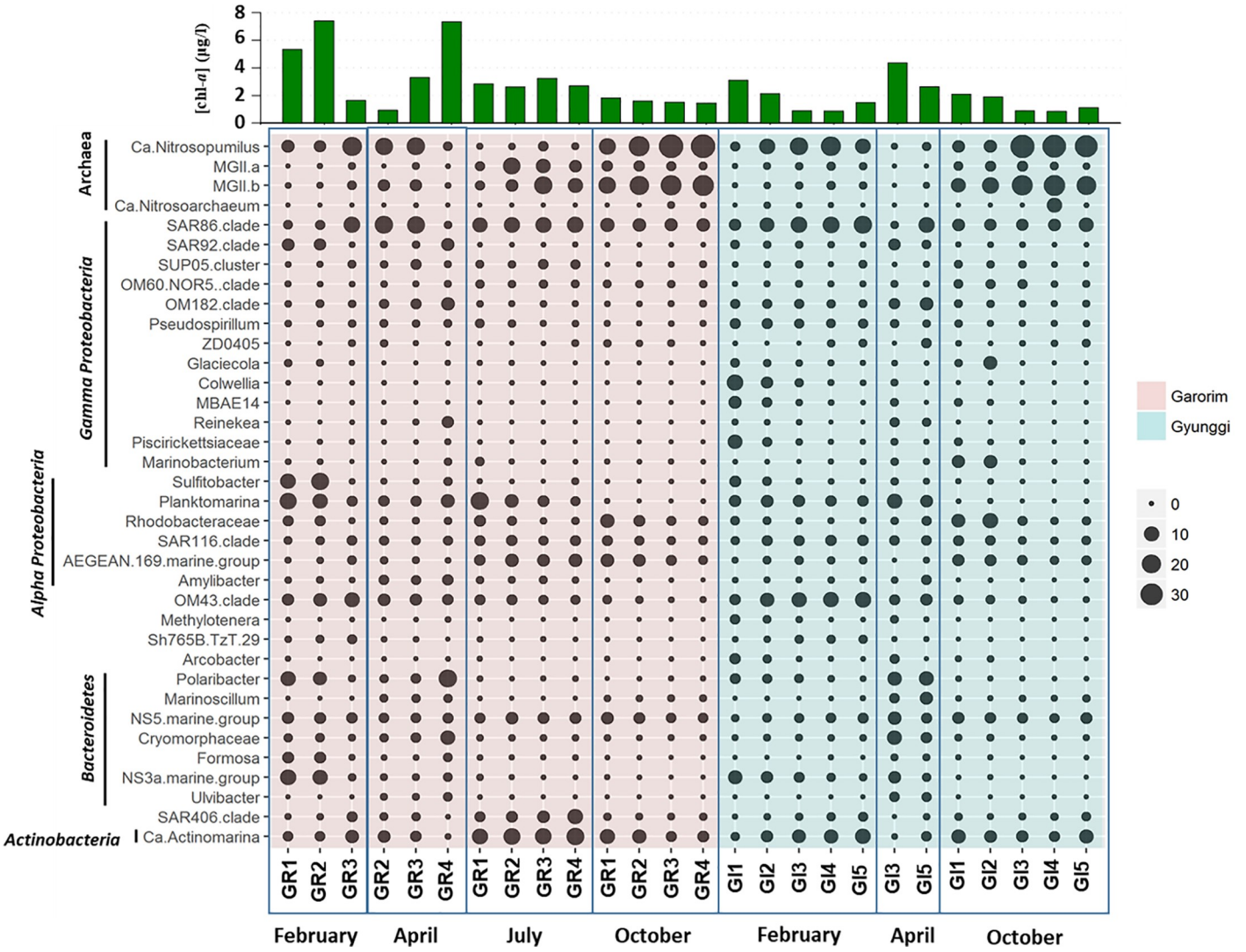

Fig 2. Taxonomic distribution of selected genera of dominant phyla of surface water microbiota in the two bays the Yellow Sea. [Chl-*a*] at each sample was shown at upper panel.

https://doi.org/10.1371/journal.pone.0221408.g002

and October samples. Archaeal abundance was shown to be slightly increasing throughout the year except for the February archaeal bloom in GR whereas the bacterial abundance showed a decreasing trend from the April bloom to October (Fig 3 and Figure A in S1 Appendix). Archaeal diversity at both bay stations showed a near-linear increase from February to October, and the highest archaeal diversity was observed at the GR stations in October (Fig 2 and Figure B in S1 Appendix). Bacterial diversities at the GI stations were relatively constant throughout the year while the GR stations showed a significantly higher diversity in April and October than in February and July.

The trends for the abundance and diversity were fit by a generalized linear model (Figure C in S1 Appendix). As expected in the temporal trends shown in Fig 3 and Figure A in S1 Appendix, the archaeal diversity and bacterial abundance closely fitted a chronological seasonal pattern (February to October). The prime predictor of archaeal diversity was the temperature, which is a good proxy for the season. The best predictor for the bacterial abundance was [chl-*a*], as expected. The archaeal diversity and bacterial abundance were modeled very well with

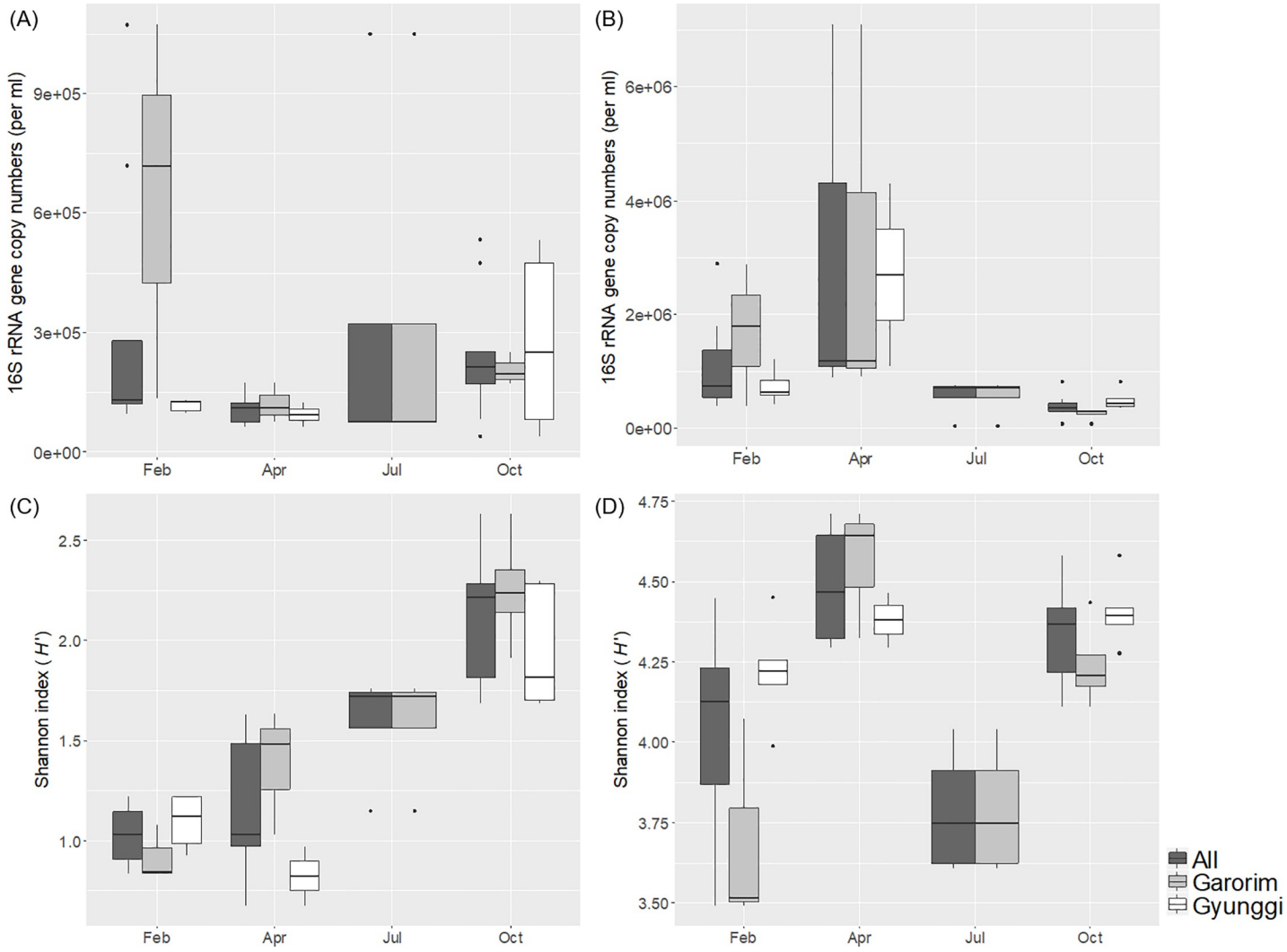

Fig 3. Box-whisker plots of abundance and diversity index per season for archaeal and bacterial assemblages measured by 16S rRNA gene qPCR and Shannon index (H') of OTU counts. (A) Archaeal abundance, (B) Bacterial abundance, (C) Archaeal diversity and (D) Bacterial diversity.

https://doi.org/10.1371/journal.pone.0221408.g003

an adjusted coefficient of determination (R_{adj}^2) over 0.5 while the archaeal abundance and bacterial diversity regression models were fitted with a lower R_{adj}^2 (<0.2). Different parameters of the archaeal and bacterial communities were modeled with different environmental variables, and the temperature, NO_2^-, and [chl-*a*] were among the consistent predictors including community structure by a redundancy analysis (RDA) and by vector fitting (Fig 4 and Table D in S1 Appendix).

Community composition and dynamics

The sequence reads were assigned to 50 described archaeal and bacterial phyla with five ubiquitous phyla making up an average of 94.9% of the reads: *Thaumarchaeota*, *Euryarchaeota*, *Proteobacteria*, *Bacteroidetes*, and *Actinobacteria* (Fig 2 and Figure D in S1 Appendix). The proportions of these five taxa in the surface seawater samples from the bay areas varied across the months; however, *Proteobacteria* were most abundant on average comprising 15%–77% of the sequence reads in all seawater samples. *Alpha-* and *Gamma-proteobacteria* were the most

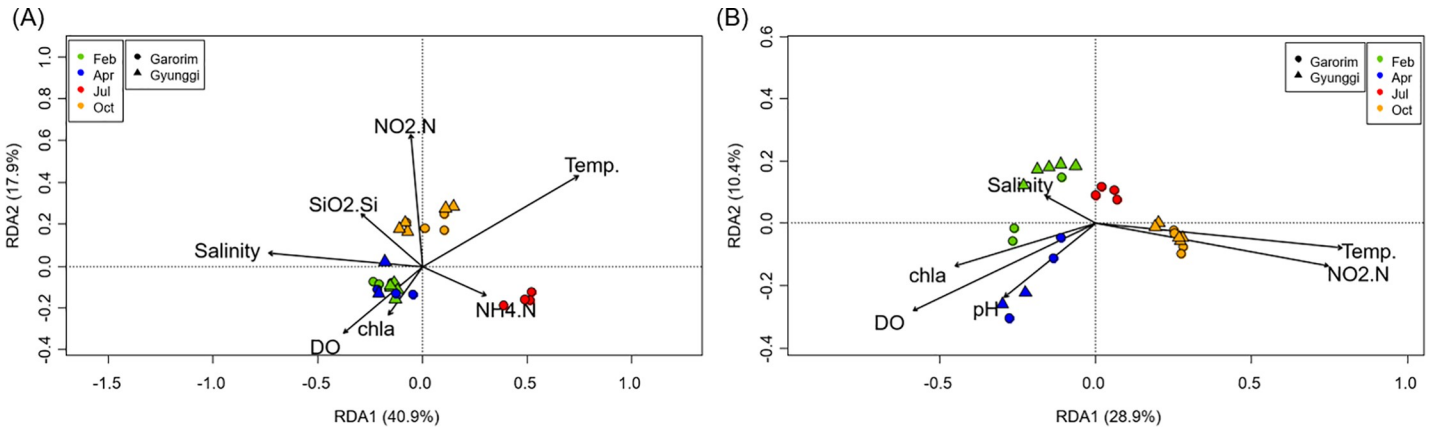

Fig 4. RDA models for archaeal (A. adj. R2 = 0.575, P = 0.001) and bacterial (B.adj.R2 = 0.410, P = 0.001) communities with selected significant environmental variables with minimum collinearity.

https://doi.org/10.1371/journal.pone.0221408.g004

abundant subphyla of the *Proteobacteria*, and the relative abundance of these groups decreased in the October samples for all but the GI1 and GI2 stations. The second most abundant group on average was *Thaumarchaeota*, which showed the opposite temporal distributional pattern to *Proteobacteria* in that the relative abundance of *Thaumarchaeota* remained relatively low from February to July and became dominant in October. The relative abundance of *Euryarchaeota*, in particular MGIIb, increased during July and October. *Bacteroidetes* were abundant during February at the GR1 and GR2 stations and in April at the GR4, GI3, and GI5 stations. *Actinobacteria* and *Marinomicrobia* (SAR406 clade) were abundant in July at the GR stations.

Although strong temporal variation was the overall trend, several taxa were identified to have clear site variations (Fig 2). At the phyla level, *Alpha-proteobacteria*, *Gamma-proteobacteria*, and *Bacteriodetes* have somewhat different patterns of relative abundance between the two bay areas. Several *Gamma-proteobacteria* taxa such as *Glaciecola*, *Colwellia*, MBAE14, *Piscirickettsiaceae*, and *Marinobacterium* were more abundant at the GI stations, especially at GI1 and GI2, which have a large freshwater influx. On the other hand, some taxa belonging to *Alpha-proteobacteria* and *Bacteroidetes*, such as *Sulfitobacter*, *Planktomarina*, *Formosa*, and NS3a marine group, were more abundant at the GR stations. Some taxa at GI1 and GI2 appear to be linked to the geochemical dynamics of the freshwater influx compared with the other sampling stations of the GI area: 1) Several bacterial taxa such as *Colwellia*, MBAE14, *Piscirickettsiaceae*, *Sulfitobacter*, *Acrobacter*, *Polaribacter*, and NS3a marine group had a higher relative abundance in the February samples while the *Glaciecola* and *Marinobacterium* relative abundance was higher in the October samples; 2) Relative abundance of the other taxa including an archaeal taxon *Ca*. Nitrosopumilus was lower in both February and October; and 3) Bacterial taxa SAR86 clade, OM43 clade, NS5 marine group, and *Ca*. Actinomarina showed a lower relative abundance in February.

Because [chl-*a*] was the prime predictor of overall bacterial abundance (Figure C in S1 Appendix), some taxa showed a clear correlation with [chl-*a*]. In GR, significant positive correlations ($\alpha < 0.05$) were found between [chl-*a*] and the relative abundances of taxa such as *Rhodobacteraceae*, *Sulfitobacter*, NS3a marine group, *Glaciecola*, NS5 marine group, and Formosa. The SUP05 cluster was negatively correlated with [chl-*a*]. In GI, significant positive correlations were found with [chl-*a*]: 1) *Alpha-proteobacteria* ($r = 0.832$, $P < 0.001$) and sub-taxa *Sulfitobacter* and SAR116 clade, 2) *Gamma-proteobacteria* ($r = 0.760$, $P = 0.004$) and sub-taxa *Pseudospirillum*, MBAE14, *Colwellia* and *Piscirickettsiaceae*, 3) *Beta-proteobacteria* ($r = 0.647$,

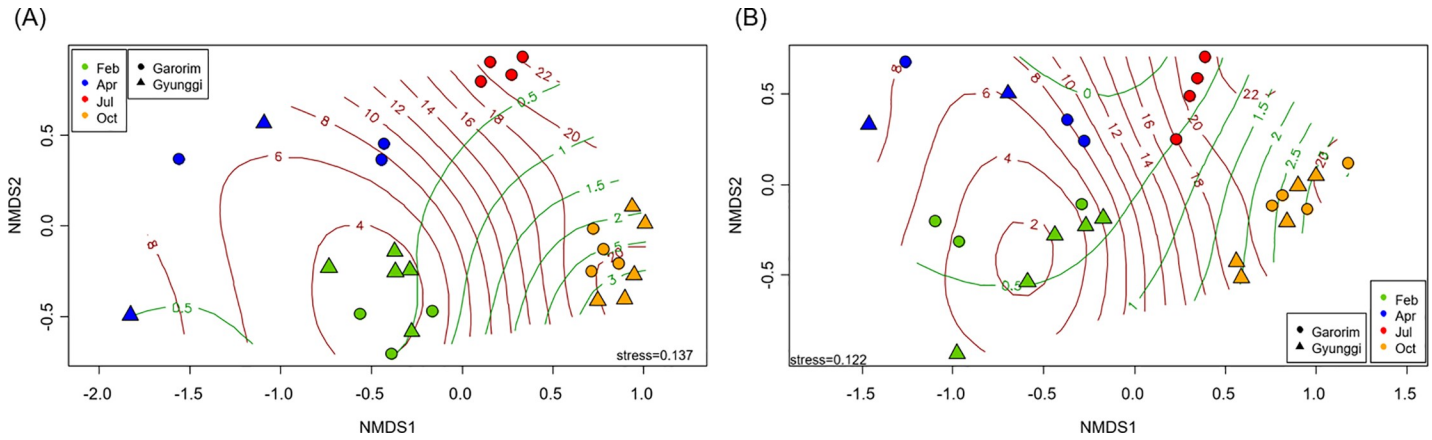

Fig 5. NMDS ordination of archaeal (A) and bacterial (B) communities with Bray-Curtis distance. Contour lines show a smooth generalized addictive model (GAM) surface reflecting best fitting environmental factors (Deviance explained: A. temperature 98.6% and NO_2^- 88.4%, and B. temperature 96.8% and NO_2^- 89.4% with $P < 0.001$ for all parameters).

https://doi.org/10.1371/journal.pone.0221408.g005

$P = 0.023$) and sub-taxa *Methylotenera* and OM43 clade. Phylum *Chloroflexi* was found to be negatively correlated with [chl-*a*] ($r = -0.700$, $P = 0.012$).

Community structure and environmental factors

Both archaeal and bacterial communities were distinctively clustered by season on the NMDS ordination (Fig 5) and tested by both ANOSIM and PERMANOVA ($P < 0.001$) (Table 1). The site distinction was shown to be not sufficiently clear. The composite environmental factors showed similar patterns to the archaeal and bacterial communities with greater overlap among the February to July samples (Figure E in S1 Appendix and Table 1). The Procrustes test and Mantel test both showed a significant association between the microbial communities and the composite environmental factors (Table E in S1 Appendix). Environmental factors were superimposed on the ordination space using generalized addictive model (GAM) surface contour instead of linear vectors for better representation of the non-linear nature of the relationship. Being top two among all environmental factors measured, the temperature and NO_2^- concentration gradients fitting the ordinations of both archaeal and bacterial communities (Fig 5) explained over 96.8% (temperature) and 88.4% (NO_2^-) of the deviance with a $P < 0.001$.

The RDA ordinations of the archaeal and bacterial communities were quite similar ($t = 0.641$, $P < 0.001$), but the RDA models built with environmental factors were quite distinctive. Archaeal communities were well explained by salinity, temperature, DO, NH_4^+, NO_2^-, SiO_2, and [chl-*a*] with 58.8% explainable variance by the first two RDA axes. Total explainable variance was 69.4%, and R_{adj}^2 is 0.575. Temperature, salinity, and NO_2^- were the top three environmental variables for the explainable variances. The February and April communities

Table 1. Permutation-based MANOVA-like analyses.

		Environmental parameters		*Archaea*		*Bacteria*	
		Month	**Site**	**Month**	**Site**	**Month**	**Site**
PERMANOVA	*F*	3.078	1.332	7.007	1.074	7.189	1.051
	P	0.002	0.246	<0.001	0.367	<0.001	0.370
ANOSIM	*R*	0.213	0.018	0.653	0.010	0.798	-0.006
	P	0.007	0.287	<0.001	0.352	<0.001	0.426

https://doi.org/10.1371/journal.pone.0221408.t001

were largely inseparable and mostly controlled by DO, [chl-*a*], and salinity. The archaeal communities in July were mostly associated with NH_4^+ while October communities were associated with NO_2^- and SiO_2. The bacterial community RDA model was built with salinity, temperature, pH, DO, NO_2^-, and [chl-*a*] with 39.7% explainable variance by the first two axes, which is less than the archaeal communities. Total explainable variance (60.4%) and R_{adj}^2 (0.449) were also lower than those of the archaeal communities. Temperature and NO_2^- were the top two environmental variables for the explainable variances. Bacterial communities were well separated per season and had distinctive environmental factors associated with them: salinity for February, pH, DO, and [chl-*a*] for April, and NO_2^- and temperature for the October samples. No environmental parameter was associated with the July bacterial communities.

Discussion

Strong seasonal variations

We investigated the temporal dynamics of archaeal and bacterial communities of two bay areas on the west coast of the Korean Peninsula. While the surface seawater archaeal and bacterial communities showed strong temporal dynamics, they were largely indistinguishable between the two bay areas. The greater temporal variation of the microbial community was supported by the strong association with environmental factors, which showed greater temporal variations than the spatial variation as well as distinctive environmental factors associated with microbial communities for different seasons (Table 1 and Figure C in S1 Appendix). Stronger temporal patterns among microbial communities rather than locations were previously observed in the New Jersey coast and the Pearl River Estuary area [35, 36].

The temporal trends for the abundance and diversity of the archaeal and bacterial communities in these two bay areas were distinct. The abundance measured by the 16S rRNA gene copy number indicated a higher average bacterial abundance than archaeal abundance, consistent with other observations [37, 38]. The diversity was estimated by calculating the Shannon index (*H*') from the OTU counts, which overall showed quite distinctive patterns compared with the 16S rRNA gene copy numbers for the abundance. Here, the comparisons we attempted to make were within each domain of the measurements and thus the difference in the abundance and diversity measures should not cause any notable problems.

Bacterial community variation

We identified the spring bloom of bacterial communities at most sampling stations, which were observed in many other previous studies as well [39–42]. Bacterial abundance was best modeled with temperature, pH, and [chl-*a*], among which pH and [chl-*a*] were more specifically associated with the bacterial communities. Bacterial abundance was higher in the April samples from both bay areas as well as the diversity (Fig 3D and Figure A in S1 Appendix). The correlated trends between abundance and diversity indicated that the spring bacterial bloom was a more community-wide phenomenon because the taxa-specific results indicate most bacterial taxa; however, most prominently, *Bacteriodetes* had an increased abundance in both bay areas. An algal bloom often drastically reduce the diversity because only a few taxa of cyanobacteria and eukaryotic algae dominate the ecosystem with the opportunity given by the input of a large quantity of nutrients and warm temperature [43, 44]. Further, in this study cyanobacteria might be underestimated because of the low binding efficiency of PCR primers with the cyanobacterial 16S rRNA gene, as suggested by Bowman and colleagues (2012).[45] Although the algal bloom was observed in April as indicated by a higher [chl-*a*], the abundant *Proteobacteria* and several newly abundant *Bacteriodetes* taxa (e.g., *Polaribacter*, *Marinoscillum*, NS5 marine group, and *Cryomorphaceae*) appeared to consistently diminish the

dominating effect by algae, and thus produced the opposite trend of a higher diversity by a higher evenness ($J'_{Apr.}$ = 0.827 and $J'_{Feb.}$ = 0.754) compared to the February samples with a comparable abundance. In the October samples, however, bacterial diversity was high while the abundance was low, potentially due to these samples having the second highest evenness ($J'_{Oct.}$ = 0.802) and a comparable richness ($S_{Oct.}$ = 1,316) to the other seasons (S_{All} = 1,445).

The temporal variation of the bacterial community composition is often driven by a few major phyla. From the current study, *Bacteroidetes* and *Alpha-proteobacteria* lead the high bacterial abundance during high [chl-*a*] seasons. *Bacteriodetes* (mainly *Polaribacter*) were dominant in February and April in both bay samples, especially when [chl-*a*] was high. Two dominant subphyla, *Alpha-proteobacteria* and *Gamma-proteobacteria*, had almost complementary relative abundance in different seasons, resulting in the consistently high abundance of *Proteobacteria* from February to July. *Alpha-proteobacteria* were more dominant at the GR stations mostly by two genera: *Sulfitobacter* and *Planktomarina*. *Sulfitobacter* and *Planktomarina* of the *Roseobacter* group have been shown to have close associations with a high [chl-*a*] [46–48]. Thus, it has been shown as a predominant community member after the peak of a bloom along with other members of the *Rhodobacteriaceae* family, as observed in the succession in nutrient-enriched marine mesocosms [49]. On the other hand, *Gamma-proteobacteria* had a higher relative abundance at the GI sites, mostly due to the SAR86 clade. Dominance of SAR86 in *Gamma-proteobacteria* year-round is unique in this area [50, 51].

Archaeal bloom

The archaeal assemblages showed a particularly strong temporal trend in these areas. While the archaeal bloom in the February samples from the GR stations had the lowest diversity, the archaeal bloom in the October samples had a higher diversity (Fig 3C and Figure B in S1 Appendix). A sudden increase in the abundance may result in either increased or decreased diversity dependent on the community composition and dynamic interactions in association with niche availability [52, 53]. Because the diversity index calculation incorporates both richness and evenness of a community, the relative importance of the diversity components can determine the overall diversity index. The October samples had the highest richness with comparable evenness among the four sampling seasons. In other words, both the *Ca*. Nitrosopumilus and MGIIb group became overly dominant (Fig 2), and the MGIIa group and *Ca*. Nitrosoarchaeum became more abundant in October than in February and April. In contrast, when a community is dominated by a few opportunistic taxa (i.e., *r* strategists), the overall diversity index may decrease because the evenness would drastically decrease, as was the case in the current study (Shannon evenness $J'_{Feb.GI}$ = 0.408). Both the October and February samples were overwhelmed by the *Ca*. Nitrosopumilus genus alone. While most inorganic nutrients were high in both the October and February samples, the temperature was much higher in October (20˚C vs. 3.6˚C), which has a general positive effect on metabolic activities, thus potentially encouraging more community-wide growth. The high input of inorganic nutrients in the GI samples in February may have promoted those fast-growing populations and thus, overall, reduced the diversity in both the archaeal and bacterial communities. Liu et al. (2018) suggested that SPM has a significant effect on the spatial distribution of *Ca*. Nitrosopumilus because of its relatedness to light penetration [54, 55]. In this study, however, the correlation between the composition of *Thaumarchaeota* and the SPM was weak, which suggests that other environmental factors may be controlling their distributions in our samples.

The relative abundance of both the *Euryarchaeota* (MGIIb group) and *Thaumarchaeota* (*Ca*. Nitrosopumilus genus) phyla overwhelmed all the other bacterial phyla in October (Fig 2), which was not common in other oceans. Furthermore, due to the single copy numbers of

the 16S rRNA gene in the genomes of both the MGIIb group (*Euryarchaeota*) and *Ca*. Nitrosopumilus (*Thaumarchaeota*) [56, 57], the relative abundance by the 16S rRNA gene copy number of archaea was likely underestimated [58]. Overall, temperature and salinity were the most important predictors for the archaeal diversity and abundance, respectively. However, the pairwise correlation analysis did not reveal any significant correlations between the relative abundance of the four most abundant archaeal taxa and environmental factors except for a weak positive correlation between *Ca*. Nitrosoarchaeum and NO_2^- ($r = 0.401$, $P = 0.042$). Note that a distinctive increase in October was observed in oxidized N species and PO_4^{3-} concentrations (Table B in S1 Appendix). The environmental factors associated with the archaeal and bacterial communities per season were somewhat similar in that temperature, salinity, and oxidized N species were common for most measured aspects between them (Fig 5 and Table B in S1 Appendix). Of course, additional environmental factors were identified to be more specific to the archaeal community such as SiO_2, SPM, DOC, and POC.

Thaumarchaeota is rarely found abundantly in the surface water of oceans and coastal seas [4, 39]. Nevertheless, we found that one of the *Ca*. Nitrosopumilus OTUs was dominant in the surface water of both bay areas. The high nitrite accumulation in the October samples may be associated with the high *Ca*. Nitrosopumilus abundance ($r = 0.769$, $P = 0.015$). One of the *Ca*. Nitrosopumilus OTUs was dominant at both bay areas. Furthermore, sequences for ammonia-oxidizing bacteria and nitrite-oxidizing bacteria were not detected at the study sites. Although the primary nitrite maximum has been suggested to be caused by algal nitrite release [59], in this study, a low [chl-*a*] and high *Ca*. Nitrosopumilus abundance ($r = -0.880$, $P = 0.002$) suggest archaeal ammonia oxidation to be a major cause of nitrite accumulation. High nitrite accumulation as observed in this study is unusual [60, 61], and may be caused by an imbalance of rates between ammonia production and nitrite oxidation.

It is interesting that MGIIb bloom is co-occurring with *Ca*. Nitrosopumilus bloom in the October samples from both bay areas (Fig 2). There were several reports of MGII bloom in oceans, and most were coastal areas. A time-series assessment of planktonic archaea in the Santa Barbara Channel revealed blooms of MGII coinciding with decreases in [chl-*a*] [62]. Another seasonal study of the surface water at the German Bight in the North Sea showed a spring bloom of MGII having >30% of the total cell counts and > 90% of all archaeal cells [63]. Galand et al. [64] speculated that the greater abundance of MGII in the Arctic Ocean may be related to the higher availability of labile organic matter from land surrounding the Arctic. In another study on the surface water of the Western Arctic, *Euryarchaeotal* abundance was very low throughout the year [65, 66] which lacked direct river inputs [67]. In contrast, in the Gyeonggi Bay area, the GI1 and GI2 stations, which were the most highly influenced by river inputs, showed a lesser archaeal abundance in both February and October. Our results coincide with the observation that brackish waters contain less archaea than seawaters [36], indicating that river inputs may not be a direct cause of archaeal blooms at these bays. The MGII group might be involved in the degradation of POC including proteins [57, 68, 69]; thus, ammonification by MGII might provide ammonia for nitrification by ammonia-oxidizing archaea, such as *Ca*. Nitrosopumilus, suggesting a co-dominance and functional coupling between the two archaeal clades.

Site-specific variations

Overall, the archaeal and bacterial community composition showed very clear temporal variations, but several taxa showed a certain degree of site variations between the two bay areas as well (Fig 2 and S3 Figure D in S1 Appendix). The changes in relative abundances of several site-specific taxa in the GI1 and GI2 station samples were significant enough to cause

substantial compositional changes at the phyla (Figure D in S1 Appendix) and OTU (Figure E in S1 Appendix) level. There were several environmental factors clearly associated with the GI1 and GI2 samples that might be direct results of a large quantity of freshwater influx: a low salinity and DO and high DIN, SPM, and POC in both the February and October samples (Table B in S1 Appendix). The site-specific taxa were not phylogenetically clustered because they spread across all phyla. With a limited number of samples, qualitative observation for the composition and relative relationship on the ordination space was attempted. NMDS achieves its configuration by positioning observations and variables into an *a priori* determined number of dimensions and preserving their relative distances among each other. The nice clustering between GI1 and GI2 and the separation from the other station samples thus ensured community distinction. Many of those taxa such as *Gamma-proteobacteria* with an altered relative abundance at the GI1 and GI2 sites might be attributable to the high freshwater influx.

In conclusion, we investigated the spatio-temporal dynamics of archaeal and bacterial communities at two geographically close bay areas on the west coast of the Korean Peninsula. Dynamic temporal changes in environmental factors observed at each station were associated with the variations in the archaeal and bacterial assemblages. The prime predictors of archaeal diversity and bacterial abundance were temperature and [chl-*a*], respectively. Temperature, NO_2^-, and [chl-*a*] were important environmental variables for both archaea and bacteria communities. Active community dynamics and population interactions resulted in complementary dominance and interesting trends in the abundance and diversity between the archaeal and bacterial populations. The archaea of the MGIIb group and *Ca*. Nitrosopumilus were co-dominant in October. There were also clear site-specific variations, especially at the stations under a freshwater influx. The distinct dynamics of the archaeal and bacterial assemblages observed in this study localized to coastal oceans were greatly affected by tides and nutrient-rich water inputs. Taken together, the results of this study provide insight into the dynamics and potential role of biogeochemistry in archaeal and bacterial communities in coastal surface seawater.

Supporting information

S1 Appendix. Supplementary results. Figure A. Abundance of archaea and bacteria in Garolim and Gyeonggi Bays measured by 16S rRNA gene qPCR. Figure B. Box-whisker plots of abundance and diversity index per bay for archaeal and bacterial assemblages measured by 16S rRNA gene qPCR and Shannon index (H') of OTU counts. (A) Archaeal abundance, (B) Bacterial abundance, (C) Archaeal diversity and (D) Bacterial diversity. **Figure C. Archaeal and bacterial abundance and diversity index along the best predictor environmental parameter fitted by generalized linear modeling (GLM).** (A) Archaeal abundance with salinity, $R_{adj}^2 = 0.190$, (B) Bacterial abundance with [chl-*a*], $R_{adj}^2 = 0.743$, (C) Archaeal diversity with temperature, $R_{adj}^2 = 0.572$ and (D) Bacterial diversity with NO_2^--NO_3^-, $R_{adj}^2 = 0.160$. **Figure D. Taxonomic distribution of the dominant phyla of surface water microbiota in Garolim and Gyeonggi Bays. Figure E. NMDS ordination of composited environmental parameters with Bray-Curtis distance. Table A. Sampling site. Table B. Environmental parameters in the sampling site. Table C. Sequence reads, richness and diversity index.** *S*: observed richness, *H*': Shannon index. **Table D. Multiple regression, vector fitting and RDA results.** Bold in multiple regression predictors indicates the most important one determined by approaches in realimpo package in R. Vector fitting was done against NMDS ordination configuration using vegan::envfit and selected with $P < 0.05$. Bold font indicates the prime predictor in GLM models (Figure C S1 Appendix). **Table E. Procrustes and Mantel test results.**
(DOCX)

Acknowledgments

We thank Hanyang University Team for their help in seawater samplings.

Author Contributions

Conceptualization: Jong-Geol Kim, Sanghoon Kang, Sung-Keun Rhee.

Data curation: Jong-Geol Kim, Sanghoon Kang.

Formal analysis: Jong-Geol Kim, Joo-Han Gwak, Sung-Uk An, Sanghoon Kang.

Funding acquisition: Sung-Keun Rhee.

Investigation: Jong-Geol Kim, Joo-Han Gwak, Man-Young Jung, Sung-Uk An.

Methodology: Jong-Geol Kim, Joo-Han Gwak, Man-Young Jung, Sung-Uk An.

Project administration: Jong-Geol Kim, Sung-Keun Rhee.

Resources: Jong-Geol Kim, Joo-Han Gwak, Man-Young Jung, Sung-Uk An, Jung-Ho Hyun, Sanghoon Kang.

Software: Jong-Geol Kim, Joo-Han Gwak, Sanghoon Kang.

Supervision: Jong-Geol Kim, Sanghoon Kang, Sung-Keun Rhee.

Validation: Jong-Geol Kim, Jung-Ho Hyun, Sanghoon Kang, Sung-Keun Rhee.

Visualization: Jong-Geol Kim, Sung-Uk An, Sanghoon Kang.

Writing – original draft: Jong-Geol Kim, Jung-Ho Hyun, Sanghoon Kang, Sung-Keun Rhee.

Writing – review & editing: Jong-Geol Kim, Jung-Ho Hyun, Sanghoon Kang, Sung-Keun Rhee.

References

1. Fuhrman JA. Microbial community structure and its functional implications. Nature. 2009; 459(7244): 193–9. https://doi.org/10.1038/nature08058 PMID: 19444205
2. Strom SL, Fredrickson KA. Intense stratification leads to phytoplankton nutrient limitation and reduced microzooplankton grazing in the southeastern Bering Sea. Deep Sea Res Part II: Topical Studies Oceanograph. 2008; 55(16): 1761–74. https://doi.org/10.1016/j.dsr2.2008.04.008
3. Fenchel. T. Azam F, Fenchel T, Field J, Gray JS, A. Meyer L, Thingstad TF. The ecological role of water-column microbes in the Sea. 1983. 257–63 p.
4. Karner MB, DeLong EF, Karl DM. Archaeal dominance in the mesopelagic zone of the Pacific Ocean. Nature. 2001; 409(6819): 507–10. https://doi.org/10.1038/35054051 PMID: 11206545
5. Francis CA, Roberts KJ, Beman JM, Santoro AE, Oakley BB. Ubiquity and diversity of ammonia-oxidizing archaea in water columns and sediments of the ocean. Proc Nat Acad Sci. 2005; 102(41): 14683–8. https://doi.org/10.1073/pnas.0506625102 PMID: 16186488
6. Ingalls AE, Shah SR, Hansman RL, Aluwihare LI, Santos GM, Druffel ERM, et al. Quantifying archaeal community autotrophy in the mesopelagic ocean using natural radiocarbon. Proc Nat Acad Sci. 2006; 103(17): 6442–7. https://doi.org/10.1073/pnas.0510157103 PMID: 16614070
7. Klawonn I, Bonaglia S, Brüchert V, Ploug H. Aerobic and anaerobic nitrogen transformation processes in N(2)-fixing cyanobacterial aggregates. ISME J. 2015; 9(6): 1456–66. https://doi.org/10.1038/ismej.2014.232 PMID: 25575306
8. Tsementzi D, Wu J, Deutsch S, Nath S, Rodriguez-R LM, Burns AS, et al. SAR11 bacteria linked to ocean anoxia and nitrogen loss. Nature. 2016; 536(7615): 179–83. https://doi.org/10.1038/nature19068 PMID: 27487207
9. Massana R, DeLong EF, Pedrós-Alió C. A few cosmopolitan phylotypes dominate planktonic archaeal assemblages in widely different oceanic provinces. Appl Environ Microbiol. 2000; 66(5): 1777–87. https://doi.org/10.1128/aem.66.5.1777-1787.2000 PMID: 10788339

10. Herndl GJ, Reinthaler T, Teira E, van Aken H, Veth C, Pernthaler A, et al. Contribution of Archaea to total prokaryotic production in the deep Atlantic Ocean. Appl Environ Microbiol. 2005; 71(5): 2303–9. https://doi.org/10.1128/AEM.71.5.2303-2309.2005 PMID: 15870315

11. Könneke M, Bernhard AE, de la Torre JR, Walker CB, Waterbury JB, Stahl DA. Isolation of an autotrophic ammonia-oxidizing marine archaeon. Nature. 2005; 437: 543–6. https://doi.org/10.1038/nature03911 PMID: 16177789

12. Martens-Habbena W, Berube PM, Urakawa H, de la Torre JR, Stahl DA. Ammonia oxidation kinetics determine niche separation of nitrifying Archaea and Bacteria. Nature. 2009; 461: 976–9. https://doi.org/10.1038/nature08465 PMID: 19794413

13. DeLong EF. Archaea in coastal marine environments. Proc Nat Acad Sci. 1992; 89(12): 5685–9. https://doi.org/10.1073/pnas.89.12.5685 PMID: 1608980

14. Hur HB, Jacobs GA, Teague WJ. Monthly variations of water masses in the Yellow and East China Seas, November 6, 1998. J Oceanogr. 1999; 55(2): 171–84. https://doi.org/10.1023/a:1007885828278

15. Lin C, Ning X, Su J, Lin Y, Xu B. Environmental changes and the responses of the ecosystems of the Yellow Sea during 1976–2000. J Mar Syst. 2005; 55(3): 223–34. https://doi.org/10.1016/j.jmarsys.2004.08.001

16. Tang Q. Changing states of the Yellow Sea large marine ecosystem: anthropogenic forcing and climate impacts in sustaining the world's large marine ecosystems, edited by Sherman K. et al., 2009. pp. 77–88, IUCN, Gland, Switzerland.

17. Turner BL. Contested identities: human-environment geography and disciplinary implications in a restructuring academy. Ann Assoc Am Geogr. 2002; 92(1): 52–74. https://doi.org/10.1111/1467-8306.00279

18. Brown MV, Philip GK, Bunge JA, Smith MC, Bissett A, Lauro FM, et al. Microbial community structure in the North Pacific ocean. ISME J. 2009; 3(12): 1374–86. https://doi.org/10.1038/ismej.2009.86 PMID: 19626056.

19. Qian PY, Wang Y, Lee OO, Lau SC, Yang J, Lafi FF, et al. Vertical stratification of microbial communities in the Red Sea revealed by 16S rDNA pyrosequencing. ISME J. 2011; 5(3): 507–18. https://doi.org/10.1038/ismej.2010.112 PMID: 20668490

20. Kirchman DL, Cottrell MT, Lovejoy C. The structure of bacterial communities in the western Arctic Ocean as revealed by pyrosequencing of 16S rRNA genes. Environ Microbiol. 2010; 12(5): 1132–43. https://doi.org/10.1111/j.1462-2920.2010.02154.x PMID: 20132284

21. Kang I, Oh H-M, Kang D, Cho J-C. Genome of a SAR116 bacteriophage shows the prevalence of this phage type in the oceans. Proc Nat Acad Sci. 2013; 110(30): 12343–8. https://doi.org/10.1073/pnas.1219930110 PMID: 23798439

22. Suzuki Y, Tanoue E, Ito H. A high-temperature catalytic oxidation method for the determination of dissolved organic carbon in seawater: analysis and improvement. Deep Sea Res Part I: Oceanogr Res Papers. 1992; 39(2): 185–98. https://doi.org/10.1016/0198-0149(92)90104-2

23. Parsons TR, Maita Y, Lalli CM. 4.3—fluorometric determination of chlorophylls. a manual of chemical & biological methods for seawater analysis. Amsterdam: Pergamon; 1984. p. 107–9.

24. Park B-J, Park S-J, Yoon D-N, Schouten S, Sinninghe Damsté JS, Rhee S-K. Cultivation of autotrophic ammonia-oxidizing archaea from marine sediments in coculture with sulfur-oxidizing bacteria. Appl Environ Microbiol. 2010; 76(22): 7575–87. https://doi.org/10.1128/AEM.01478-10 PMID: 20870784

25. Park S-J, Park B-J, Rhee S-K. Comparative analysis of archaeal 16S rRNA and amoA genes to estimate the abundance and diversity of ammonia-oxidizing archaea in marine sediments. Extremophiles. 2008; 12(4): 605–15. https://doi.org/10.1007/s00792-008-0165-7 PMID: 18465082

26. Roesch LFW, Fulthorpe RR, Riva A, Casella G, Hadwin AKM, Kent AD, et al. Pyrosequencing enumerates and contrasts soil microbial diversity. ISME J. 2007; 1: 283–90. https://doi.org/10.1038/ismej.2007.53 PMID: 18043639

27. Lane DJ, Pace B, Olsen GJ, Stahl DA, Sogin ML, Pace NR. Rapid determination of 16S ribosomal RNA sequences for phylogenetic analyses. Proc Nat Acad Sci. 1985; 82(20): 6955–9. https://doi.org/10.1073/pnas.82.20.6955 PMID: 2413450

28. Caporaso JG, Kuczynski J, Stombaugh J, Bittinger K, Bushman FD, Costello EK, et al. QIIME allows analysis of high-throughput community sequencing data. Nat methods. 2010; 7(5): 335–6. https://doi.org/10.1038/nmeth.f.303 PMID: 20383131

29. Aronesty E. Comparison of sequencing utility programs. Open Bioinforma J. 2013; 7(1): 1–8. https://doi.org/10.2174/1875036201307010001

30. Aronesty E. ea-utils: "Command-line tools for processing biological sequencing data. 2011.

31. Edgar RC. Search and clustering orders of magnitude faster than BLAST. Bioinformatics. 2010; 26 (19): 2460–1. https://doi.org/10.1093/bioinformatics/btq461 PMID: 20709691

32. DeSantis TZ, Hugenholtz P, Larsen N, Rojas M, Brodie EL, Keller K, et al. Greengenes, a chimera-checked 16S rRNA gene database and workbench compatible with ARB. Appl Environ Microbiol. 2006; 72(7): 5069–72. https://doi.org/10.1128/AEM.03006-05 PMID: 16820507

33. Team RC. R: A language and environment for statistical computing. R Foundation for Statistical Computing, Vienna, Austria. 2016. https://www.R-project.org/

34. Marra G, Wood SN. Practical variable selection for generalized additive models. Computational Statistics and Data Analysis. 2011; 55(7): 2372–87. https://doi.org/10.1016/j.csda.2011.02.004

35. Nelson JD, Boehme SE, Reimers CE, Sherrell RM, Kerkhof LJ. Temporal patterns of microbial community structure in the Mid-Atlantic Bight. FEMS Microbiol Ecol. 2008; 65(3): 484–93. https://doi.org/10.1111/j.1574-6941.2008.00553.x PMID: 18662312

36. Xie W, Luo H, Murugapiran SK, Dodsworth JA, Chen S, Sun Y, et al. Localized high abundance of Marine Group II archaea in the subtropical Pearl River Estuary: implications for their niche adaptation. Environ Microbiol. 2018; 20(2): 734–54. https://doi.org/10.1111/1462-2920.14004 PMID: 29235710

37. Yin Q, Fu B, Li B, Shi X, Inagaki F, Zhang X-H. Spatial variations in microbial community composition in surface seawater from the ultra-oligotrophic center to rim of the South Pacific Gyre. PLoS One. 2013; 8 (2): e55148. https://doi.org/10.1371/journal.pone.0055148 PMID: 23405118

38. Liu H, Zhang CL, Yang C, Chen S, Cao Z, Zhang Z, et al. Marine Group II dominates planktonic archaea in water column of the Northeastern South China Sea. Front Microbiol. 2017; 8(1098). https://doi.org/10.3389/fmicb.2017.01098 PMID: 28663746

39. Needham DM, Fuhrman JA. Pronounced daily succession of phytoplankton, archaea and bacteria following a spring bloom. Nat Microbiol. 2016; 1:16005. https://doi.org/10.1038/nmicrobiol.2016.5 PMID: 27572439

40. Teeling H, Fuchs BM, Becher D, Klockow C, Gardebrecht A, Bennke CM, et al. Substrate-controlled succession of marine bacterioplankton populations induced by a phytoplankton bloom. Science. 2012; 336(6081): 608–11. https://doi.org/10.1126/science.1218344 PMID: 22556258

41. Larsen A, Flaten GAF, Sandaa R-A, Castberg T, Thyrhaug R, Erga SR, et al. Spring phytoplankton bloom dynamics in Norwegian coastal waters: microbial community succession and diversity. Limnol Oceanogr. 2004; 49(1): 180–90. https://doi.org/10.4319/lo.2004.49.1.0180

42. Liu M, Xiao T, Sun J, Wei H, Wu Y, Zhao Y, et al. Bacterial community structures associated with a natural spring phytoplankton bloom in the Yellow Sea, China. Deep Sea Res Part II: Topical Studies Oceanograph. 2013; 97: 85–92. https://doi.org/10.1016/j.dsr2.2013.05.016

43. Sison-Mangus MP, Jiang S, Kudela RM, Mehic S. Phytoplankton-associated bacterial community composition and succession during toxic diatom bloom and non-bloom events. Front Microbiol. 2016; 7. https://doi.org/10.3389/fmicb.2016.01433 PMID: 27672385

44. Elliott JA, May L. The sensitivity of phytoplankton in Loch Leven (UK) to changes in nutrient load and water temperature. Freshwat Biol. 2008; 53(1): 32–41. https://doi.org/10.1111/j.1365-2427.2007.01865.x

45. Bowman JS, Rasmussen S, Blom N, Deming JW, Rysgaard S, Sicheritz-Ponten T. Microbial community structure of Arctic multiyear sea ice and surface seawater by 454 sequencing of the 16S RNA gene. ISME J. 2012; 6(1): 11–20. https://doi.org/10.1038/ismej.2011.76 PMID: 21716307

46. Grossart H-P, Levold F, Allgaier M, Simon M, Brinkhoff T. Marine diatom species harbour distinct bacterial communities. Environ Microbiol. 2005; 7(6): 860–73. https://doi.org/10.1111/j.1462-2920.2005.00759.x PMID: 15892705

47. Sapp M, Wichels A, Gerdts G. Impacts of cultivation of marine diatoms on the associated bacterial community. Appl Environ Microbiol. 2007; 73(9): 3117–20. https://doi.org/10.1128/AEM.02274-06 PMID: 17369346

48. Sapp M, Schwaderer AS, Wiltshire KH, Hoppe H-G, Gerdts G, Wichels A. Species-specific bacterial communities in the phycosphere of microalgae? Microb Ecol. 2007; 53(4): 683–99. https://doi.org/10.1007/s00248-006-9162-5 PMID: 17264999

49. Allers E, Gómez-Consarnau L, Pinhassi J, Gasol JM, Šimek K, Pernthaler J. Response of Alteromonadaceae and Rhodobacteriaceae to glucose and phosphorus manipulation in marine mesocosms. Environ Microbiol. 2007; 9(10): 2417–29. https://doi.org/10.1111/j.1462-2920.2007.01360.x PMID: 17803768

50. Treusch AH, Vergin KL, Finlay LA, Donatz MG, Burton RM, Carlson CA, et al. Seasonality and vertical structure of microbial communities in an ocean gyre. ISME J. 2009; 3(10): 1148–63. https://doi.org/10.1038/ismej.2009.60 PMID: 19494846

51. Milici M, Deng Z-L, Tomasch J, Decelle J, Wos-Oxley ML, Wang H, et al. Co-occurrence analysis of microbial taxa in the Atlantic Ocean reveals high connectivity in the free-living bacterioplankton. Front Microbiol. 2016; 7(649). https://doi.org/10.3389/fmicb.2016.00649 PMID: 27199970

52. O'Dwyer JP, Kembel SW, Green JL. Phylogenetic diversity theory sheds light on the structure of microbial communities. PLoS Comput Biol. 2012; 8(12): e1002832. https://doi.org/10.1371/journal.pcbi.1002832 PMID: 23284280

53. Coyte KZ, Schluter J, Foster KR. The ecology of the microbiome: networks, competition, and stability. Science. 2015; 350(6261): 663–6. https://doi.org/10.1126/science.aad2602 PMID: 26542567

54. Merbt SN, Stahl DA, Casamayor EO, Martí E, Nicol GW, Prosser JI. Differential photoinhibition of bacterial and archaeal ammonia oxidation. FEMS Microbiol Lett. 2012; 327(1): 41–6. https://doi.org/10.1111/j.1574-6968.2011.02457.x PMID: 22093004

55. Liu Q, Tolar BB, Ross MJ, Cheek JB, Sweeney CM, Wallsgrove NJ, et al. Light and temperature control the seasonal distribution of thaumarchaeota in the South Atlantic bight. ISME J. 2018; 12(6): 1473–85. https://doi.org/10.1038/s41396-018-0066-4 PMID: 29445129

56. Walker CB, de la Torre JR, Klotz MG, Urakawa H, Pinel N, Arp DJ, et al. Nitrosopumilus maritimus genome reveals unique mechanisms for nitrification and autotrophy in globally distributed marine crenarchaea. Proc Nat Acad Sci. 2010; 107(19): 8818–23. https://doi.org/10.1073/pnas.0913533107 PMID: 20421470

57. Iverson V, Morris RM, Frazar CD, Berthiaume CT, Morales RL, Armbrust EV. Untangling genomes from metagenomes: revealing an uncultured class of marine Euryarchaeota. Science. 2012; 335(6068): 587–90. https://doi.org/10.1126/science.1212665 PMID: 22301318

58. Sun D-L, Jiang X, Wu QL, Zhou N-Y. Intragenomic heterogeneity of 16S rRNA genes causes overestimation of prokaryotic diversity. Appl Environ Microbiol. 2013; 79(19): 5962–9. https://doi.org/10.1128/AEM.01282-13 PMID: 23872556

59. Collos Y. Nitrate uptake, nitrite release and uptake, and new production estimates. Marine Ecology Progress Series. 1998; 171: 293–301. https://www.jstor.org/stable/24831744

60. Chow C-ET, Sachdeva R, Cram JA, Steele JA, Needham DM, Patel A, et al. Temporal variability and coherence of euphotic zone bacterial communities over a decade in the Southern California Bight. ISME J. 2013; 7(12): 2259–73. https://doi.org/10.1038/ismej.2013.122 PMID: 23864126

61. Wuchter C, Abbas B, Coolen MJL, Herfort L, van Bleijswijk J, Timmers P, et al. Archaeal nitrification in the ocean. Proc Nat Acad Sci. 2006; 103(33): 12317–22. https://doi.org/10.1073/pnas.0600756103 PMID: 16894176

62. Murray AE, Blakis A, Massana R, Strawzewski S, Passow U, Alldredge A, et al. A time series assessment of planktonic archaeal variability in the Santa Barbara Channel. Aquat Microb Ecol. 1999; 20(2): 129–45. https://doi.org/10.3354/ame020129

63. Pernthaler A, Preston CM, Pernthaler J, DeLong EF, Amann R. Comparison of fluorescently labeled oligonucleotide and polynucleotide probes for the detection of pelagic marine bacteria and archaea. Appl Environ Microbiol. 2002; 68(2): 661–7. https://doi.org/10.1128/AEM.68.2.661-667.2002 PMID: 11823205

64. Pierre EG, Connie L, Warwick FV. Remarkably diverse and contrasting archaeal communities in a large arctic river and the coastal Arctic Ocean. Aquat Microb Ecol. 2006; 44(2): 115–26. https://doi.org/10.3354/ame044115

65. Kirchman DL, Elifantz H, Dittel AI, Malmstrom RR, Cottrell MT. Standing stocks and activity of archaea and bacteria in the western Arctic Ocean. Limnol Oceanogr. 2007; 52(2): 495–507. https://doi.org/10.4319/lo.2007.52.2.0495

66. Alonso-Sáez L, Sánchez O, Gasol JM, Balagué V, Pedrós-Alio C. Winter-to-summer changes in the composition and single-cell activity of near-surface Arctic prokaryotes. Environ Microbiol. 2008; 10(9): 2444–54. https://doi.org/10.1111/j.1462-2920.2008.01674.x PMID: 18557769

67. Galand PE, Lovejoy C, Pouliot J, Vincent WF. Heterogeneous archaeal communities in the particle-rich environment of an arctic shelf ecosystem. J Mar Syst. 2008; 74(3): 774–82. https://doi.org/10.1016/j.jmarsys.2007.12.001

68. Martin-Cuadrado A-B, Garcia-Heredia I, Moltó AG, López-Úbeda R, Kimes N, López-García P, et al. A new class of marine Euryarchaeota group II from the mediterranean deep chlorophyll maximum. ISME J. 2014; 9(7): 1619–34. https://doi.org/10.1038/ismej.2014.249 PMID: 25535935

69. Orsi WD, Smith JM, Liu S, Liu Z, Sakamoto CM, Wilken S, et al. Diverse, uncultivated bacteria and archaea underlying the cycling of dissolved protein in the ocean. ISME J. 2016; 10(9): 2158–73. https://doi.org/10.1038/ismej.2016.20 PMID: 26953597.